Vitesse d'adhésion de cellules bactériennes sur du sable : propriété de surface et vitesse d'adhésion.

Le chapitre 2 correspond à l'article

Kinetic adhesion of bacterial cells to sand:

Cell surface properties and adhesion rate.

Colloids and Surfaces B : Biointerfaces, volume 59 (2007), p. : 35-45

A. Jacobs, F. Lafolie, J.M. Herry et M. Debroux

Avant propos

Comme on pu le constater dans le chapitre état de l'art, l'adhésion des cellules bactériennes sur un support joue un rôle important dans leur transport en milieu poreux. La littérature montre l'implication des propriétés de surface des cellules et de la phase solide dans ce phénomène. Par propriétés de surface on entend les propriétés physicochimiques (hydrophobicité et charge électrique de la surface cellulaire et du support). De nombreux auteurs ont utilisé la théorie DLVO pour quantifier les interactions physicochimiques entre cellules bactériennes et un support solide avec plus ou moins de succès. Cependant la plupart des études se sont focalisées sur quelques souches bactériennes seulement (essentiellement *E. coli*, *P. aeroginosa* et *Bacillus subtilis*) avec des propriétés de surface assez proches. Aussi dans cet article nous avons voulu étudier la relation entre l'adhésion (sur du sable) et les interactions physicochimiques d'un large panel de bactéries. Le choix des souches s'est effectué afin d'obtenir une gamme étendue de propriété physicochimiques. La très grande diversité microbiologique des stations d'épuration laisse supposer aussi une grande diversité au niveau des caractéristiques de surface cellulaire. L'objectif de cette étude était donc de quantifier l'adhésion de bactéries à un solide bien défini et d'évaluer par le biais de la théorie DLVO dans quelle mesure l'adhésion (quantité et cinétique) peut être reliée à leurs propriétés physicochimiques de surface.

Available online at www.sciencedirect.com
ScienceDirect
Colloids and Surfaces B: Biointerfaces 59 (2007) 35–45
COLLOIDS AND SURFACES B
www.elsevier.com/locate/colsurfb

Kinetic adhesion of bacterial cells to sand: Cell surface properties and adhesion rate

A. Jacobs [a], F. Lafolie [a,*], J.M. Herry [b], M. Debroux [a]

[a] *I.N.R.A., Unité Climat Sol Environnement, Bâtiment Sol, Domaine Saint-Paul, Site Agroparc, 84914 Avignon Cedex 9, France*
[b] *UMR I.N.R.A. E.N.S.I.A., Bioadhésion et Hygiène des Matériaux, 25 Avenue de la République, 91744 Massy Cedex, France*

Received 12 January 2007; received in revised form 28 March 2007; accepted 11 April 2007
Available online 24 April 2007

Abstract

Correlation between microbial surface thermodynamics using the extended DLVO (XDLVO) theory and kinetic adhesion of various bacterial cells to sand was investigated. Two experimental setups were utilized. Adhesion tests were conducted in batch reactors with slow agitation. Also, bacteria were circulated through small sand columns in a closed loop and the results were analyzed with a simple model which accounted for the rate of the adhesion phenomena (ω in h^{-1}) and adhesion percentage. Cells surface properties were derived from contact angle measurements. The wicking method was utilized to characterize the sand. Zeta potentials were measured for the sand and the cells. Kinetic of bacterial retention by the porous media was largely influenced by the electrostatic interactions which are correlated with ω from the model ($R^2 = 0.71$). Negative zeta potentials resulted in electrostatic repulsions occurring between the sand and the bacterial cells which in result delayed bacterial adhesion. While no correlation was found between the adhesion percentage and the total interaction energy calculated with the XDLVO theory the respective behavior of hydrophobic and hydrophilic bacteria as well as the importance of electrostatic interactions was evidenced. All the bacterial strains studied adhered more in the column experiments than in the adhesion tests, presumably due to enhanced collision efficiency and wedging in porous media, while filtration could be ignored except for the larger *Bacillus* strains. Approximate XDLVO calculations due to solid surface nanoscale roughness, retention in a secondary minimum and population heterogeneity are discussed. Our results obtained with a large variety of different physicochemical bacterial strains highlights the influence of both surface thermodynamics and porous media related effects as well as the limits of using the XDLVO theory for evaluating bacterial retention through porous media.

Keywords: Bacteria; Adhesion; Transport; Sand; XDLVO

1. Introduction

The transport and fate of microbial particles in subsurface environments is a significant stake in both bioremediation and drinking water contamination [1]. The consequences related to the displacement of bacterial cells in the soil can cause many environmental [2–7], agronomic [8] and health related problems [9]. Several contaminations of water sources with micro-organisms were most likely due to bacterial transport through the unsaturated zone [3]. However the displacement of micro-organisms in a soil profile is still poorly understood. Increasing experimental evidences suggest that bacterial transport is strongly influenced by cell characteristics [10]. Cell surface physicochemical properties and its biochemical composition seem to be closely related to the surface thermodynamics which are well known to play an important role in cell to solid surface interactions which will affect bacterial transport [11,12]. Marshall and colleagues [13] in a pioneering work were the first to use the classical Derjaguin–Landau–Verwey–Overbeek (DLVO) theory to describe microbial adhesion to solid surfaces. The DLVO theory has been widely used since that time to estimate the net interaction between bacteria cells and inert surfaces resulting from the addition of Lifshitz–van der Waals (LW) and electrostatic interactions (EL). Later Van Oss developed the extended DLVO theory (XDLVO) by adding the Lewis acid–base interactions (AB) [14]. The polar Lewis acid–base or electron-acceptor/electron-donor interactions are responsible for all non-electrostatic, non-covalent, polar interactions occurring in water [15]. LW, AB and EL interactions can be influenced by cell modifications and properties such as the physicochemi-

* Corresponding author. Tel.: +33 4 32 72 22 16; fax: +33 4 32 72 22 12.
E-mail address: jacobs@avignon.inra.fr (F. Lafolie).

0927-7765/$ – see front matter © 2007 Elsevier B.V. All rights reserved.
doi:10.1016/j.colsurfb.2007.04.008

cal state [16], extracellular polymeric substance (EPS) [17–19], C/N ratio in nutrients [20], lipopolysaccharides (LPS) production [21,22], motility [23,24] or shape [25]. The surface of living cells is chemically complex and heterogeneous which complicates the physicochemical approach for the comprehension of bacterial adsorption phenomena on a solid surface. It has already been demonstrated that hydrophobicity, which can be described by AB interactions for biological compounds, is the driving force for bacterial deposition and is usually one order of magnitude greater than EL or LW interactions [26,27]. However contradictory reports show that correlation between the XDLVO theory and bacterial transport can either be good [28,29] or poor [30,31]. Although not investigated in this paper, physical factors (porous media, temperature, flow velocity) and chemical factors (ionic strength, ion species, pH) are also well known for their impact on bacterial adsorption mechanisms.

Predicting the transport of bacterial cells or colloids in a porous media requires the attachment and detachment processes as well as the straining and liberation mechanisms to be modeled. Most studies [12,28] employ transport models based on the convection dispersion with various types of adhesion sites. Usually, one type is assumed to be instantaneously and reversibly in equilibrium with the aqueous concentration leading to the concept of retardation factor [28]. Adsorption on other sites is kinetic, and can be reversible or not [12]. The latter process is often referred as *deposition* and the coefficient controlling its rate is usually fitted together with other parameters (partition coefficients for equilibrium and kinetic site types) so that the model correctly reproduces the observed breakthrough curves [28]. The deposition coefficient can also be simply obtained experimentally from the fraction of micro-organisms recovered at the outlet of the soil column [32]. This method was used by Chen and Strevett [27]. As pointed out by Tufenkji et al. [33], the deposition factor may vary with time and space due to coverage of solid particle by attaching cells; which modifies the interactions between the cells and the porous medium. Chen and Strevett [27,28] and Chen et al. [34] reported laboratory experiments that clearly illustrate that bacterial cells transport through porous medium is largely controlled by adhesion (instantaneous and kinetic) and also that the deposition coefficient varies from a bacteria to another. In addition, they found that the total free energy of interaction evaluated by the DLVO was correlated with the deposition coefficient obtained from their column experiments.

In this study we are interested to further investigate how surface properties of a large number of bacteria influence attachment kinetics to sand. This work differs from previous column experiments in that a large variety of strains with different physicochemical properties (i.e. hydrophobicity and electrophoresis characteristics) were used. Our goal was to relate the rate of adhesion and the percentage of adhesion to Lifshitz–van der Waals, Lewis acid–base and electrostatic interactions. The impact of cell size and shape on retention in the porous media was also analyzed. In order to measure porous media related effects on bacterial adsorption, simple adhesion tests (batch with gentle agitation) and small column experiments were compared. Our goal is also to evaluate the possibility of using an experimental setup that requires less time and work than a traditional column experiment for evaluating bacterial cells deposition in a porous medium.

2. Materials and methods

2.1. Bacterial strains and solid phase

All the bacterial strains and their origins used in this work are listed in Table 1. Some of the strains listed are uncommon to soil environments such as bacteria from the *Streptococcus* and the *Lactococcus* families but their particular membrane properties (i.e. hydrophobicity and low zeta potential) were chosen in order to obtain a large variety of cell surface characteristics. All the *Streptococcus* strains were kindly given by the National Institute for Agricultural Research in Paris (INRA, France). The *L. lactis* NDCO2118 strain used in this study was isolated from frozen peas and was given by the National Collection of Dairy Organisms (France). Cell size measurements were performed with a Canon BX microscope. Results are listed in Table 1.

The bacteria were grown in half diluted Luria–Bertani (1/2LB) media or M17 with 10% lactose media for the lactic acid bacteria at 30 °C. The bacteria were first cultivated in 10 ml of their respective media for 6 h. About 0.1 ml of the first culture was used to inoculate 50 ml of 1/2LB or M17 and incubated for overnight culture.

The porous media used in this study was a sand called "sand of Fontainebleau" (south Paris, France) (Merck, grain size: Ø 230–310 μm). This sand is very homogeneous (over 99.6% silica) and is composed of quartz grains. Before use, the sand was thoroughly rinsed with milliQ water on a 40 μm filter (VWR international, 11 cm, type 417) then heat treated and oven dried for at least 2 h at 120 °C. For each experiment the sand was renewed in the columns.

2.2. Surface properties of cells and porous medium

Bacterial and sand surface thermodynamic properties can be described by their surface energy. According to the extended DLVO theory, bacterial and sand surface tension is mainly composed of an apolar component (i.e. Lifshitz–van der Waals: LW), a polar component (i.e. Lewis acid/base: AB) and an electrical component (EL) [35]:

$$\Delta G = \Delta G^{AB} + \Delta G^{LW} + \Delta G^{EL}$$

Attraction between two surfaces occurs when ΔG is negative and repulsion occurs when ΔG is positive. Bacterial LW and AB components of surface energy were estimated by contact angle measurements following the method described by Grasso et al. [36]. The Dupré–Young equation relates the contact angle made by a drop of liquid (L) deposited on a flat solid (S), to the surface energy and the interfacial tension of the liquid and the flat solid:

$$(1 + \cos\theta)\gamma_L = 2\left(\sqrt{\gamma_S^{LW}\gamma_L^{LW}} + \sqrt{\gamma_S^{+}\gamma_L^{-}} + \sqrt{\gamma_S^{-}\gamma_L^{+}}\right) \quad (1)$$

Table 1
GRAM, size and source of the bacterial strains used in this study

Strains	GRAM (G) and known particularity	Size[a]	Source or reference
Azospirillum lipoferum Sp59b^T	G−	4.2/1	Collection[b]
Azospirillum brasilense Sp7^T	G−	2.7/1.1	Collection[b]
Bacillus cereus LMG 69	G+	4.6/1.6	Collection[b]
Bacillus subtilis LMG	G+	10.8/1.6	Collection[b]
E. coli K-12 PHL565*gfp*	(Curlis production +)	1.2/0.5	Collection[c]
E. coli K-12 PHL1314	Mutant ompR234 (curlis production ++)	1.2/0.5	Collection[c]
L. lactis NDCO2118	G+	0.85	Collection[d]
Pantoea agglomerans ATCC 27155^T	G−	4/1	Collection[b]
Paenibacillus graminis RSA19^T	G+	5.3/1	Collection[b]
Paenibacillus polymyceae CF43	G+	5.2/1	Collection[b]
Paenibacillus polymyceae SBO3	G+	4.7/1	Collection[b]
Pseudomonas corrugata ATCC 29736^T	G−	1.7/0.5	Collection[b]
Pseudomonas fluorescens AK15	G−	2.8/1	Collection[e]
Rahnella aquatilis ATCC33071^T	G−	1.2	Collection[b]
S. salivarius JIM8777	G+	1.2	Collection[d]
S. salivarius JIM8780	G+	1	Collection[d]
S. thermophilus CNRZ1066	G+	1.1	Collection[d]
S. thermophilus LMG18311	G+	1	Collection[d]
S. thermophilus JIM8732	G+	1	Collection[d]
S. thermophilus JIM8752	G+	1	Collection[d]
S. thermophilus JIM8749	G+	1	Collection[d]

[a] Cell sizes are in μm, the rod shaped cells are indicated by length/width, cocci shaped cells by their diameter.
[b] Strains listed in Table 1 were kindly provided by O. Berge (CEA Cadarache, France).
[c] Strains listed in Table 1 were kindly provided by P. Lejeune (INSA LYON, France).
[d] Strains listed in Table 1 were kindly provided by P. Renault (INRA Jouy en Josas, Paris, France).
[e] Strains listed in Table 1 were kindly provided by Y. Dudal (INRA Avignon, France).

where the subscripts S and L indicate the solid (bacteria) and the liquid, respectively, θ the contact angle (°) between the bacterial layer and the liquid, γ_L the surface energy of the liquid used for the measurement (mJ m^{-2}), γ^{LW} the Lifshitz–van der Waals component of the surface energy (mJ m^{-2}), and γ^+ and γ^- are the electron-acceptor and the electron-donor parameters of the Lewis acid/base component of surface energy (mJ m^{-2}). The liquid surface energy γ_L is calculated as

$$\gamma_L = \gamma_L^{LW} + \gamma_L^{AB} = \gamma_L^{LW} + 2\sqrt{\gamma_L^+ \gamma_L^-} \quad (2)$$

Water, 1-bromonaphtalene and formamide (Sigma–Aldrich, MO, USA) were used to obtain three contact angles. Their Lifshitz–van der Waals and Lewis acid base properties are listed in Table 2. Bacterial cells collected from the stationary growth state were first centrifuged (5 min, 5000 rpm), washed and suspended in 0.01 M NaCl and then vacuum filtered trough nitrocellulose membranes filters (0.45 μm, type HA, Millipore®, USA) to create a bacterial layer. For each strain three contact angle measurements per liquid were performed on two bacterial layers obtained from separate cultures. Contact angles were measured with a G40 goniometer (Krüss, Palaiseau, France). For each strain, mean measured contact angles were used in equation [1] to calculate the γ^{LW}, γ^+ and γ^- components of the surface energy.

Table 2
The surface free energies components of MATS solvents and contact angle liquids

Liquids	γ^{LW} (mJ m^{-2})	γ^{AB} (mJ m^{-2})	γ^+ (mJ m^{-2})	γ^- (mJ m^{-2})
Water	21.8	51.0	25.5	25.5
Formamide	39.0	19.0	39.6	2.3
1-bromonaphtalen	44.4	0	0	0
Chloroform	27.2	3.8	3.8	0
Hexadecane	27.2	0	0	0
Decane	23.9	0	0	0
Ethyl acetate	23.9	19.4	0	19.4

Lifshitz–van der Waals and Lewis acid–base component of the surface energy for the sand were obtained by the wicking method. The wicking method consists in measuring the progression of the wetting front as a function of time during a capillary liquid penetration experiment. The Washburn equation describes the position of the wetting front as a function of liquid and porous media properties:

$$h^2 = (R_e t \gamma_L \cos\theta)(2\mu)^{-1} \quad (3)$$

where R_e (m) is the average pore radius, t the time (s), h(m) the height of capillary rise of the wicking liquid, μ (N s m^{-2}) the viscosity of the liquid, θ the contact angle between the liquid and the solid and γ_L (mJ m^{-2}) is the liquid surface energy. The mean pore radius was estimated with a liquid such that $\cos\theta = 1$ (i.e. hexadecane). Next, measurements were made with three liquids to obtain three values of θ and Eq. (1) was used to calculate the components of the surface tension of the solid. For each liquid, ten measurements were carried out. For each experiment, the contact angle is calculated by fitting Eq. (1) to experiments. Our setup was made of small glass tubes ($L = 10$ cm, $\emptyset = 0.5$ cm) filled with the sand. The weight of the liquid absorbed by the sand was measured as a function of time to obtain the liquid capillary rise velocity.

ζ potentials (V) of bacteria were determined by microelectrophoresis using a Zetaphoremeter model (II) (CAD Instrumentation, Limours, France). The electrophoretic mobility was measured with the bacteria collected after overnight culture, suspended in a 0.01 M NaCl of pH 7 solution at room temperature. Bacterial cells were placed in a measurement cell under a microscope equipped with a CCD camera. Their displacements in response to an applied electric field of 8 V cm^{-1} were recorded and the velocity of individual cells was calculated. The ζ potentials were calculated with the conventional Smoluchowski theory for each cell. The displacements of about one hundred cells were recorded at each measurement. For each strain, the experiment was made three times from separate cultures. The electro kinetic properties of the sand were measured by a streaming potential analyzer Zetacad (CAD Instrumentation, Limours, France) in a 0.01 M NaCl of pH 7 solution. The zeta potential was calculated from the streaming potential experiments as described by Elimelech et al. [37].

2.3. Evaluation of hydrophobicity: MATS method

The MATS method has been described in detail previously [38]. Briefly this method is based on the comparison between microbial affinity to a monopolar solvent and a apolar solvent. The two solvents must have the same Lifshitz–van der Waals component of surface energy. The monopolar solvent can be either acidic (electron acceptor) or basic (electron donor). *n*-Alkane solvents have neither electron donor nor electron acceptor properties. The following pairs of polar and non-polar solvents were selected on the basis of the MATS method requirements:

- Chloroform, an acidic solvent (electron acceptor) and hexadecane, an *n*-alkane.
- Ethyl acetate, a strongly basic solvent (electron donor) and decane, an apolar solvent.

All solvents used in this study were obtained from Sigma–Aldrich (MO, USA) and were of the highest purity grade (99.9%). The surface properties of the liquids used in this study are listed in Table 2. The MATS method was performed in a high ionic strength solution to avoid the influence of electrostatic interactions [38]. Experimentally, 2.4 ml of a 0.1 M potassium phosphate buffer was vortex-mixed with 0.4 ml of the solvent under investigation for 90 s. To ensure complete separation of the two phases the mixture stands at rest for 15 min before a sample of 2 ml was removed from the aqueous phase and its absorbance measured at 400 nm. The affinity of microbial cells to a solvent was calculated by

$$\%\text{adhesion} = \left(\frac{1 - A}{A_0}\right) \times 100 \quad (4)$$

where A_0 is the absorbance of the aqueous phase at 400 nm before mixing and A is its absorbance after mixing.

2.4. Kinetic of bacterial cells adhesion to sand

The experimental setup consisted in a small Plexiglas column (Ø = 18 mm, length = 33 mm) filled with the sand. For all the experiments and strains, the column was filled with 13.38 g of dry sand leading to a porosity of 0.4. Next the column was saturated with sterilized water (0.01 M NaCl of pH7) (3.4 mL). Physical factors (porosity, flow rate, temperature) and chemical factors (ionic strength, pH) remained constant for all the experiments. Bacterial cells were collected during the stationary growth stage, centrifuged for 5 min at 5000 rpm and suspended in a sterile 0.01 M solution of NaCl with pH = 7. Prior to use, 10 ml of solution (0.01 M NaCl, pH = 7) with bacterial concentrations in the range of 10^6 to10^7 cells ml^{-1} was prepared. Circulation of this bacterial solution in a closed loop through the column was obtained by mean of a peristaltic pump Ismatec SA reglo digital MS-4 (Switzerland). The flow rate was 3.5 mL min^{-1} which allowed a mean residence time in the column lower than 1 min. Consequently, the bacterial concentration in the solution could be assumed uniform throughout the column and hydrodynamic effects could be ignored. Bacterial concentration in the batch solution was measured by taking 0.5 ml samples at the following times during the experiment: 0, 1, 2, 4, 6, 8, 10, 15, 20 and 30 min. Each sample was stained with a nucleic acid dye (Bacterial counting kit, B-7277, Molecular Probes) for flow cytometer enumeration. The flow cytometer (Beckman Coulter, EPIC XL) settings were as follows: excitation source 488 nm, fluorescence detection on FL1 channel (emission 510–530 nm), analysis time 1 min, no compensation was used.

2.5. Adsorption study: batch adhesion tests

Because physical straining can be an important factor in bacterial retention by porous media, we also carried out adsorption tests where filtration could not occur. The same settings were used as in the column experiments: 13.68 g of sand was mixed for 30 min with 10 ml of a bacterial solution in 50 ml Falcon® tubes. This solution (0.01 M NaCl, pH = 7) had a bacterial concentration of about 10^7 cells ml^{-1}. Tubes were placed horizontally in an orbital shaker running at 60 rpm. A control was prepared as for the samples described above but without the sand. Cell counting using the cytometer (as described in the column experiments section) was performed at the beginning and at the end of the experiment.

3. Theory

3.1. The free energy of interaction

$\Delta G_{y_0}^{LW}$ and $\Delta G_{y_0}^{AB}$ are the Lifshitz–van der Waals and Lewis acid/base free energy of interaction between the bacteria (1) and a sand grain (2) immersed in water (3) at closest approach (y_0). $\Delta G_{y_0}^{LW}$ can be calculated with the following equation:

$$\Delta G_{y_0}^{LW} = -2\left(\sqrt{\gamma_3^{LW}} - \sqrt{\gamma_2^{LW}}\right)\left(\sqrt{\gamma_3^{LW}} - \sqrt{\gamma_1^{LW}}\right) \quad (5)$$

and $\Delta G_{y_0}^{AB}$ can be evaluated by

$$\Delta G_{y_0}^{AB} = 2\left(\sqrt{\gamma_1^+\gamma_3^-} + \sqrt{\gamma_2^+\gamma_3^-} + \sqrt{\gamma_1^-\gamma_3^+} + \sqrt{\gamma_2^-\gamma_3^+} - \sqrt{\gamma_1^+\gamma_2^-} - \sqrt{\gamma_1^-\gamma_2^+} - 2\sqrt{\gamma_3^+\gamma_3^-}\right) \quad (6)$$

The electrostatic interaction free energy as a function of distance y between a spherical bacterium (1), and a flat plate sand grain (2), immersed in water (3) can be calculated from the following equation [28]:

$$\Delta G_{132}^{EL}(y) = \pi R\varepsilon_r\varepsilon_0\left(2\psi_{01}\psi_{02}\ln\left(\frac{1+e^{-ky}}{1-e^{-ky}}\right) + (\psi_{01}^2+\psi_{02}^2)\ln(1-e^{-2ky})\right) \quad (7)$$

where ε and ε_0 are the relative dielectric permittivity of water (78.55 at 25 °C) and permittivity under vacuum ($8.854.10^{-12}$ C mV^{-1}), respectively, R the bacterial radius (m), $1/\kappa$ the Debye–Hückel length, y the distance between the spherical bacterium and the flat plate sand grain (m), and ψ_{01} and ψ_{02} are the potentials at the bacterial and the sand surfaces estimated by [35]:

$$\psi_0 = \zeta\left(\frac{1+z}{R}\right)e^{\kappa z} \quad (8)$$

with ζ is the zeta potential (V) measured at the slipping plate, z the distance measured from the particle surface to the slipping plate (m) and R is the radius of the particle. The length z is generally of the order of 0.5 nm [35]. The Debye–Hückel length (or double layer thickness), k^{-1} value is 3.2 nm in a 0.01 M solution of a 1:1 salt which was used here. EL interactions were calculated at a distance of 6.4 nm corresponding to the electric double layers of both the sand grains and the bacterial cell.

3.2. Modelling the batch experiment

Several approaches have been used when modeling cells adsorption on a solid. The filtration theory has been widely used [12,28]. This approach assumes that the rate of bacterial cells deposition on the solid is proportional to the cell concentration in the fluid. The deposition coefficient incorporates porous media characteristics, flow velocity and cells surface properties by means of a collision efficiency factor. This model assumes irreversible adhesion of cells. Transport models incorporating the filtration model, also use a retardation factor which means that instantaneous and reversible adsorption sites are also present [12,28]. So, these models are in fact two-sites type models with one type of sites being kinetic and irreversible and the other type being instantaneous and reversible. Chen et al. [34] used a model with a retardation factor and with reversibility of adsorption for kinetic sites. In their model, the first-order rate coefficient is identical for adsorption and detachment.

In our case, we suppose that adsorption occurs only on sites for which adsorption is kinetic and reversible. At any time the following mass balance equation is verified:

$$(V_p + V_b)C(t) + MS(t) = C_0V_b \quad (9)$$

where $C(t)$ (cells ml^{-1}) is the concentration in the aqueous phase, $S(t)$ the concentrations of bacteria immobilized on the solid (cell g^{-1}), M (g) the amount of solid, V_p (ml) the volume of solution in the porosity of the small column initially free of cells and V_b (ml) is the external volume of solution containing the cells at the beginning of experiments. C_0 is the initial concentration of the batch solution. Upon derivation of Eq. (9) with respect to time one has

$$V_t\frac{dC}{dt} + M\frac{dS}{dt} = 0 \quad (10)$$

where we noted $V_t = V_p + V_b$. Assuming that deposition of bacteria on the solid is reversible and obeys a first-order equation we have

$$\frac{dS}{dt} = \omega(kC - S) \quad (11)$$

where ω (h^{-1}) is the first-order rate constant and k (cm^3 g^{-1}) is the partition constant. From Eq. (9), the following expression for S is obtained:

$$S(t) = \frac{V_bC_0}{M} - \frac{V_t}{M}C(t) \quad (12)$$

Using Eqs. (11) and (12) in Eq. (10) we get the following ordinary differential equation relating the changes of the concentration in the solution to the adsorption process:

$$\frac{dC}{dt} = -\frac{A}{V_t}C(t) + \frac{B}{V_t} \quad (13)$$

with $A = \omega(V_t + kM)$ and $B = \omega V_bC_0$. The solution of this equation is then:

$$C(t) = \left(C_0 - \frac{B}{A}\right)e^{-At/V_t} + \frac{B}{A} \quad (14)$$

The solution was used with a least-squares minimization algorithm to evaluate parameters ω and k.

4. Results

4.1. Zeta potential

All strains showed negative ζ-potentials in these conditions but varied from −0.5 to −48 mV (Table 3). Most ζ-potentials determined here are in agreement with those reported in other studies. In general bacterial cells are negatively charged in a low ionic solution of pH 7. It is well known that ζ-potentials of living cells are modified by ionic strength [39,40] and/or the pH [41,42] of the environment but this was not investigated in our study. No significant differences were observed between Gram positive and Gram negative cells although some gram positive bacteria were the only to show ζ-potentials close to zero.

Table 3
The surface free energies components and zeta potentials for the bacterial strains studied and the sand

Strains	ζ (mV)	S.D. ζ	γ^+	γ^-	γ^{LW}	ΔG^{LW}	ΔG^{AB}	ΔG^{EL}	ΔG^{AB+LW}	Col[a]	Adh[a]	k	ω (h^{-1})
Azospirillum lipoferum Sp59b^T	−11.15	0.36	2.78	53.59	31.74	−0.63	10.42	1.29	9.78	78.5	52.0	4	10
Azospirillum brasilense Sp7^T	−15	0.43	2.74	53.48	32.07	-0.65	10.36	1.71	9.70	88.0	54.7	6	7.56
Bacillus cereus LMG69	−27.25	1.28	1.35	51.45	36.81	-0.92	8.97	4.93	8.05	95.0	0.0	22	5.25
Bacillus subtilis LMG	−31.5	0.90	0.80	56.00	44.60	-1.32	10.60	3.76	9.28	95.0	0.0	37	4.23
E. coli K-12 PHL565gfp	−48.86	0.37	0.98	54.18	38.28	-1.00	9.94	5.67	8.95	29.0	3.5	1	2.33
E. coli K-12 PHL1314	−44.5	0.99	0.72	51.98	40.34	−1.10	8.86	6.30	7.76	23.4	0.0	1	2.18
L. lactis NDCO2118	−14.52	0.93	1.53	50.00	35.99	−0.87	8.42	1.65	7.54	46.8	30.8	1	2.68
Pantoea agglomerans ATCC 27155T	−23.45	0.74	0.57	55.51	32.72	−0.69	10.25	2.74	9.56	95.0	44.0	21	9.22
Paenibacillus graminis RSA19^T	−23.05	0.68	2.46	54.69	30.78	−0.58	10.77	2.69	10.20	81.0	40.7	4	7.13
Paenibacillus polymyceae CF43	−5.6	0.09	1.46	65.15	29.76	−0.52	14.56	0.82	14.05	13.0	0.0	1	9.14
Paenibacillus polymyceae SBO3	−5.45	0.15	1.66	63.98	29.51	−0.50	14.20	0.77	13.70	13.0	0.0	1	9.62
Pseudomonas corrugata ATCC 29736^T	−14.5	0.83	4.06	55.70	31.00	−0.59	11.67	2.71	11.08	96.0	64.0	35	4.04
Pseudomonas fluorescens AK15	−23.43	0.39	1.37	57.15	36.20	−0.88	11.36	2.19	10.48	95.0	63.9	171	7.11
Rahnella aquatilis ATCC33071^T	−25.3	1.22	0.86	56.42	37.45	−0.95	10.81	2.97	9.85	36.0	21.8	1	6.08
S. salivarius JIM8777	−13.96	0.37	2.28	20.23	40.70	−1.12	−7.18	1.63	−8.30	100.0	89.0	1000	9.79
S. salivarius JIM8780	−15.31	0.32	2.18	20.35	41.00	−1.14	−7.14	0.91	−8.27	100.0	89.5	1000	10.21
S. thermophilus CNRZ1066	−3.29	0.41	1.51	42.06	36.73	−0.91	4.79	0.15	3.88	99.1	74.4	635	10.28
S. thermophilus LMG18311	−0.4	0.87	1.68	41.86	36.50	−0.90	4.77	−0.01	3.87	97.6	74.0	184	10
S. thermophilus JIM8732	−27.64	0.32	2.26	22.28	39.04	−1.04	−5.82	0.00	−6.85	100.0	91.2	802	13.68
S. thermophilus JIM8752	−2.44	0.30	1.72	47.20	36.73	−0.91	7.26	−0.02	6.34	100.0	76.0	794	12.7
S. thermophilus JIM8749	−1.11	1.24	1.34	52.77	37.01	−0.93	9.53	0.26	8.60	98.6	72.0	664	8.48
Porous media													
sand	−42.11		3.85	20.4	24.97								

Results for free energies of interaction between bacteria and sand are listed as ΔG^{LW}, ΔG^{AB}, ΔG^{EL} and ΔG^{AB+LW} (mJ m^{-2}). Results for column experiments, batch adhesion tests and fitted parameters from the model are, respectively, listed as Col, Adh, k and ω.

[a] "Col" and "Adh", respectively, corresponds to the percentage of cell adhesion in the Column experiments and the Adhesion tests. γ^+, γ^-, γ^{LW}, ΔG^{LW}, ΔG^{AB}, ΔG^{LW+AB} and ΔG^{EL} are expressed in mJ m^{-2}. k is the partition constant at equilibrium (cm^3 g^{-1}).

4.2. Hydrophobic and hydrophilic character of bacterial cells

Fig. 1 presents the adhesion of bacterial cells to various solvents-interfaces obtained with the MATS method. Most of the strains studied showed higher affinity for chloroform than for hexadecane whereas their adhesion to ethyl acetate was generally very low. Thus these results indicated that the microbial cells surfaces were strongly electron donating and weakly electron accepting, leading to the concept of "monopolar surfaces" [43]. Only four strains (i.e. *S. salivarius* JIM8780 and JIM8077, *S. thermophilus* JIM8032 and *P. corrugata*) adhered strongly to hexadecane and to decane and appeared to be very hydrophobic. Several strains (i.e. *Bacillus cereus* and *Bacillus subtilis*, *Lactococcus lactis* NDCO2118 as well as *Paenibacillus polymyceae* CF43 and SB03) had very low affinity for all the hydrophobic solvents used in this study which means that their cell surface were the most hydrophilic of all the strains studied. The bacterial strains studied were mainly hydrophilic as they adhered less than 40% to the non-polar solvents used.

4.3. Bacterial and sand thermodynamic properties

Bacterial and sand surface thermodynamic properties obtained with the contact angle measurements and the wicking method are listed in Table 3. Most of the strains showed a strong electron donating character with high γ^- values around 50 mJ m^{-2} and with a small γ^+ electron acceptor component. These results are in agreement with the concept of monopolar particles which is often used to qualify bacterial cells. Both *S. salivarius* strains and *S. thermophilus* JIM8732 appeared to be hydrophobic according to the contact angle measurements. This is also in agreement with the results of the MATS method. A biological surface is considered to be hydrophobic when both electron donating and accepting characters γ^- and γ^+ are greater or lesser than those of water (i.e. $\gamma^-_{water} = \gamma^+_{water} = 25.5$ mJ m^{-2}) [26]. Only *P. corrugata* which is hydrophobic according to our MATS results appeared as hydrophilic with the contact angle experiments. Sand from Fontainebleau (South Paris, France) is composed of quartz particles and was slightly hydrophilic (Table 3).

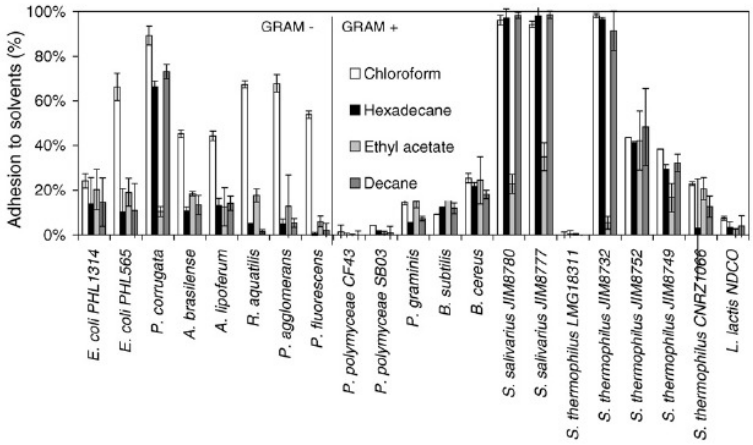

Fig. 1. Results for the MATS method obtained with chloroform (white), hexadecane (black), ethyl acetate (grey light) and decane (grey). The standard deviation (bars) was calculated from 4 measurements realized on two independent cultures. Gram negative bacteria are presented on the left, Gram positive bacteria are on the right. (For interpretation of the references to colour in this figure legend, the reader is referred to the web version of the article.)

Free energy of interaction between bacterial cells and the sand was estimated using Eqs. (5)–(7) in order to calculate the LW, AB and EL components (Table 3). LW interactions showed negative values for all the bacterial strains and therefore contribute to bacterial adhesion to the sand. Interestingly only the hydrophobic cells showed negative ΔG^{AB} values in contrast with hydrophilic strains which showed positive AB interactions. The addition of LW and AB interaction at 0.157 nm (distance of closest approach according to Van Oss [35]) was noted as ΔG^{LW+AB}. As it can be seen from Table 3, ΔG^{LW+AB} varied from −8.30 to 14.05 mJ m^{-2}. Hydrophobic strains (*S. thermophilus* JIM8732, and both *S. salivarius* JIM8780 and JIM8777) were the only bacteria with negative ΔG^{LW+AB} values in the range −8.30 to −6.85 mJ m^{-2}. ΔG^{EL} calculated at 6.4 nm (Eq. (5)) was nearly always positive (ranging from 0 to 6.30 mJ m^{-2}) which promoted repulsion between the cells and the sand.

4.4. Batch experiments

Fig. 2 shows three contrasted examples of measured bacterial cell log concentrations during the column experiments as a function of time and their respective reproductions by the model. For all the strains, concentrations displayed kinetics similar to those presented. Differences between strains are: i/ the rate of concentration decrease in the solution (parameter ω in the model) and ii/ the concentration reached when the steady state is achieved (parameter k in the model). Some species disappeared nearly completely from the solution (e.g. *S. salivarius* JIM8777, *S. salivarius* JIM8780, all of the *S. thermophilus* strains). Others species reached an equilibrium concentration larger than 0.

Fitting the parameters k and ω in Eq. (14) provided a good restitution by the model of observations whatever the species. Fitted parameters are given in Table 3. The higher the value of k the more bacteria were retained by the sand matrix. The parameter k varied from 0.54 to 1000 cm^3 g^{-1}. Hydrophobic strains showed the highest k values (from 802 to 1000 cm^3 g^{-1}) while bacteria with zeta potentials close to zero showed k values from 170 to 796 cm^3 g^{-1}. Hydrophilic strains with zeta potentials under −5 mV showed k values lower than 40 cm^3 g^{-1} (except *P. fluorescence*). Thus the hydrophobic strains were the best retained by the sand, followed by low charged cells while hydrophilic cells with low zeta potentials adhered the least to the porous media.

Parameter ω represents the first-order rate constant for the retention process. The higher ω the faster bacteria adhered to the sand matrix. Values for ω varied from 2.18 to 13.68 h^{-1} (Table 3). The largest ω values, i.e. strains that adhered the fastest, corresponded to bacteria that have the largest ζ-potentials (*A. lipoferum* for example), while strains with the lowest ζ-potentials (*E. coli* for example) where retained more slowly.

As predicted with the XDLVO theory hydrophobic and/or low charged bacteria are better retained by the sand matrix than highly negatively charged hydrophilic bacteria. However according to our results ΔG^{TOT} ($\Delta G^{AB} + \Delta G^{LW} + \Delta G^{EL}$) was

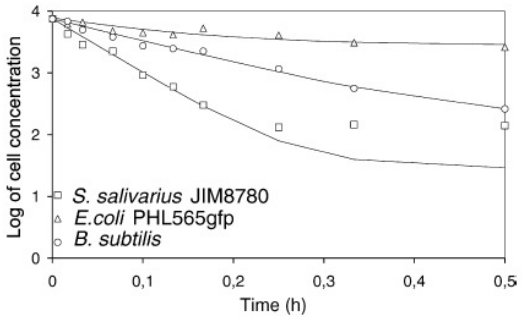

Fig. 2. Three contrasted examples of evolution of the bacterial cell concentration in the batch solution. Experimental results are respectively represented by the squares (*S. salivarius* JIM8780), circles (*B. subtilis*) and triangles (*E. coli* PHL565gfp). Full lines correspond to the fitted models of each strain.

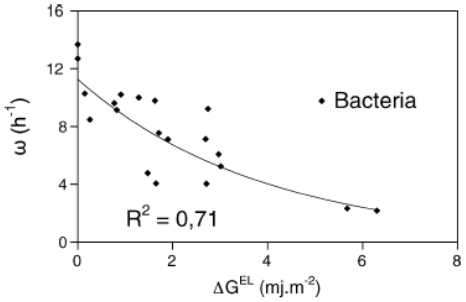

Fig. 3. Correlation between potential zeta (mV) and the first-order rate constant ω^{-1} (min). Curve shows the correlation for the eye.

always positive (i.e. repulsive) for hydrophilic cells which mean that adhesion on the sand matrix should theoretically never happen. Despite this repulsive energy barrier adhesion to sand of hydrophilic cells occurred in both batch adhesion tests and column experiments which is discussed in detail in the Discussion section.

4.5. Correlations

We looked for correlations between the bacterial/sand thermodynamic properties (variables ΔG^{LW+AB} and ΔG^{EL}) and the adhesion percentage and ω (rate of adhesion) obtained from columns and adhesion tests experiments. A significant correlation was found between ω and ΔG^{EL} ($R^2 = 0.71$, $p < 0.0001$) (Fig. 3): low zeta potentials of both bacterial cells and sand particles resulted in higher ΔG^{EL} values (i.e. the electrostatic barrier) which delayed adhesion with lower ω values (rate of adhesion).

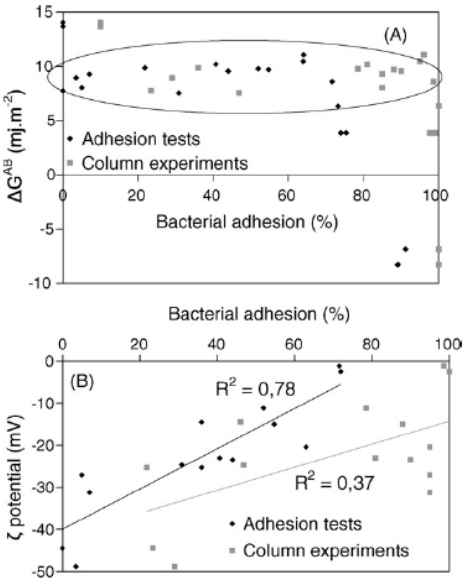

Fig. 4. (A) ΔG^{AB} as a function of bacterial adhesion (%) on sand during the adhesion tests (black boxes) and the column experiments (grey squares). Bacteria with similar ΔG^{AB} values are represented inside the circle. (B) ζ potential (mV) as a function of bacterial adhesion (%) on sand during the adhesion tests (black boxes) and the column experiments (grey squares) for bacteria with similar ΔG^{AB} values. (For interpretation of the references to colour in this figure legend, the reader is referred to the web version of the article.)

Fig. 4A shows the relation between the percentage of adhesion and ΔG^{LW+AB} for both types of adhesion experiments (column and batch). From Fig. 4A: most bacterial strains showed similar ΔG^{LW+AB} around 10 mJ m^{-2} but very different adhesion behaviours. Both *P. polymyceae* CF43 and SB03 had the highest ΔG^{LW+AB} values (14 mJ m^{-2}) and the lowest adhesion percentage to sand, whereas the *S. salivarius* strains and *S. thermophilus* JIM8732 strains had the lowest ΔG^{LW+AB} (around -8 mJ m^{-2}) and the highest adhesion percentage. So it seems that only extreme values of ΔG^{LW+AB} influence significantly the adhesion. Interestingly, the ζ-potentials enabled to explain adhesion percentage differences among the bacterial cells displaying similar ΔG^{LW+AB} values. In Fig. 4B the zeta potential of the 14 strains with similar ΔG^{LW+AB} values was plotted with their respective adhesion percentages in both adhesion and column experiments. The zeta potential was well correlated with the adhesion percentage obtained from the batch adhesion experiments ($R^2 = 0.77$, $p < 0.0001$), despite a less significant correlation with the results obtained from the small column experiments ($R^2 = 0.37$, $p < 0.0001$).

5. Discussion

5.1. Adhesion percentage

Our hydrophobic strains have a negative total energy of interaction with the solid and display a high percentage of adhesion. This is in agreement with the extended DLVO theory and with Van Oss [15] who pointed out the importance of "hydrophobic attraction" between hydrophobic and hydrophilic surfaces in aqueous media. The calculated total energy of interaction was positive for all our hydrophilic bacteria. Although adhesion of hydrophilic cells on sand occurred in our experiments, which do not agree with the theory, we noted these bacterial strains had less affinity for the sand than the hydrophobic strains. Similar results have been observed in other studies [44,45] Hence, our results show that, for strains with negative and low ΔG^{AB} values bacterial adhesion is eased, whereas a positive high ΔG^{AB} obstructs bacterial adhesion to the sand matrix but without fully preventing it (Fig. 4A). Retention of bacteria in porous media under unfavourable conditions has already been observed for particular strains [46]. Several mechanisms have been proposed to explain this: straining, solid particle roughness effects, retention in a secondary energy minimum or heterogeneity of the population.

5.2. Straining

According to Bradford et al. [47] filtration occurs when particle diameter is higher than 5×10^{-3} times the mean diameter of porous media grains. Using this criteria with our porous material, bacterial cells with a diameter smaller than 1.5 μm should

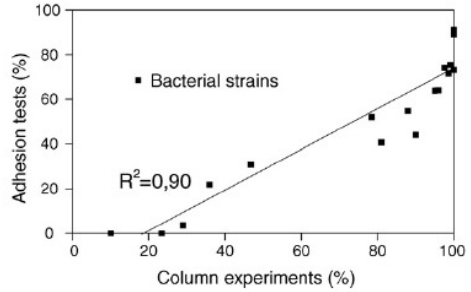

Fig. 5. Correlation (linear regression) between the results obtained with adhesion tests and the column experiments. Note that the results for the *Bacillus* strains are not included as those bacteria were likely retained by filtration during the column experiments.

not be strained. *Bacillus* strains set apart, all the bacteria studied were thinner than 1.5 μm (Table 1) and thus filtration should be minimal. Some of our cells are rod shaped and as long as 5 μm. Previous studies report filtration for long rod-shaped cells [10,25]. However, in our case, we observed that rod shaped cells such as *P. polymyceae* strains (5 μm long and 1 μm thick) were very little retained in our column experiments. Thus we think that filtration should be negligible for any smaller cells, which is the case for all of the other strains used except the *Bacillus* strains. For the largest bacteria (i.e. the *Bacillus* strains were 5–10 μm long and 1.5–2 μm thick) filtration might have occurred and be the main cause for retention. In deed, *Bacillus subtilis* and *Bacillus cereus* did not stick to sand particles in the batch adhesion tests but 95% of the cells were retained in the column experiments. Not considering *Bacillus* strains for which straining was important, adhesion percentages measured with the two methods for all others bacteria are linearly correlated with a determination coefficient of 0.9 (Fig. 5). The good correlation found between the adhesion and column experiments for the adhesion percentage suggests that filtration was certainly not the main factor for bacterial retention in our column experiments.

Still the adhesion percentage was always higher in the column experiments than in the batch adhesion tests (Table 3). We believe that enhanced collision efficiency in the column experiments (bacterial cells travelled through the column about 30 times increasing probability to encounter sand grain surfaces) and several porous media related effects such as wedging (discussed hereafter) may explain the better adhesion evidenced in the column experiments. So, i/ our observations are consistent with the results predicting filtration from the size of soil particles and cells (Bradford et al.) and ii/ the comparison of the two types of experiment allows to conclude that, for all the strains except the largest, retention of cells in the porous media is not due to filtration.

5.3. Nanometer and micrometer roughness of sand particles

Some authors pointed out the effect of surface roughness (nanometer scale) on DLVO calculations [48–50]. In our calculations of the free energy of interaction, we considered the

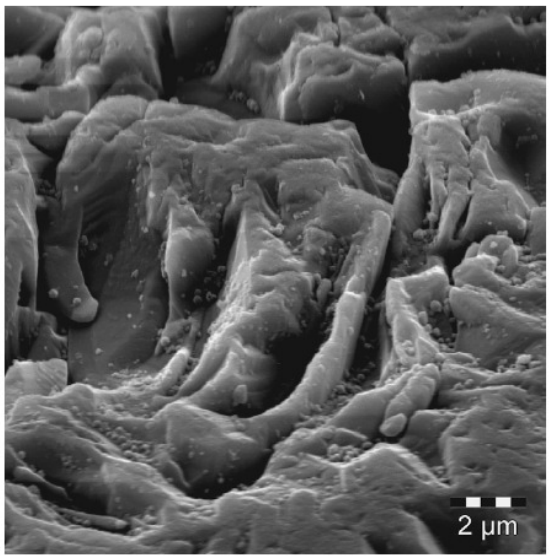

Fig. 6. Roughness of a Fontainebleau sand grain used in this study. Observation performed with a scanning electron microscope. "Caves" and "valleys" on bacterial cell scale are possible locations where bacteria can be trapped inside and prevent their transport.

bacterial cells as perfectly smooth spheres and the sand grains as flat planes as assumed by the XDLVO theory. Hoek and Agarwal [49] found that surface roughness causes significant reduction in the repulsive (or attractive) interaction energy. Surface heterogeneities create greater particle-substrate separation distance which causes the reduction of interaction energy. The authors concluded that because the generally attractive LW interactions are stronger at long range, (where both AB and EL interactions are negligible or null) rough surfaces might be favorable for colloid deposition.

Moreover mechanical trapping of cells by sand grains interstices during the column experiments are possible phenomena that may explain bacterial retention on the sand matrix without involvement of XDLVO interactions [51]. Sand grain topography on a microscopic scale (i.e. bacterial cell scale) is made of "valleys" and "caves" as it can be seen from Fig. 6. Bacteria may be blocked inside these asperities. Cells might also be trapped by sand grain-grain junction as Bradford et al. recently pointed out [52]. Also, Johnson and colleagues simulated colloids behaviour at a microscale in a porous media by means of a model accounting for the various forces experienced by the particles [53]. They showed that colloid retention in presence of an energy barrier could happen due to wedging and retention in zones of flow stagnation [53]. The better adhesion found in our column experiments (compared to the adhesion tests) might be explained by their findings (Fig. 5).

5.4. Secondary energy minimum

Redman et al. pointed out the importance of LW interactions in bacterial transport through porous media [46]. LW interac-

tions are generally negative (i.e. attractive) long range forces that can act up to 25 nm from the surface which provide the secondary minimum where bacteria can be "trapped". At such distances AB interactions are null and EL interactions negligible. The calculated secondary energy minimum for our conditions (porous medium, cells and ionic strength) are located at about 30 nm from the solid surface and range from −0.2 to −1 kT with most values close to −0.5 kT which is of about (2×10^{-21} mJ m^{-2}). These values are low and similar to values calculated by Redman et al. for *E. coli* at an ionic strength of 0.01 M. In such conditions Redman et al. observed a high percentage of detachment when a 0.1 mM solution was applied [46]. They attributed this high percentage of detachment to the retention of their cells in the secondary minimum. To evaluate to which extend retention of our cells was due to secondary minimum, we selected five bacteria with surface charges spanning the whole range of our set of strains: *E. coli* (−48 mV), *R. aquatilis* (−25.3 mV), *A. brasilense* (−15 mV), *S. salivarius* JIM8777 (−14 mV) and *S. thermophilus* CNRZ1066 (−3.2 mV) to carry out detachment experiments. At the end of the attachment mini-column experiments, the solution was removed and replaced by milliQ water which was circulated though the columns for 30 min after what the concentration of cells in the solution was measured. These experiments showed that the amount of cells detached amounted to 25, 10 and 12% of previously attached cells for *E. coli*, *R. aquatilis* and *A. brasilense*, respectively. These percentages are significantly lower than those obtained by Redman et al. with a strain displaying a surface charge similar to ours. Due to very weak electrostatic repulsion, the low charged bacteria *S. thermophilus* CNRZ1066 (−3.2 mV) was not detached when the ionic strength was lowered. *S. salivarius* JIM8777 displayed negative AB interactions with sand (Table 3) which means it is likely firmly retained in the primary minimum. So the observed absence of detachment was expected and the result is in accordance with the measured characteristics of the strain. In light of these results, we believe that, in our conditions, and the hydrophobic bacteria set apart, retention in the secondary minimum is only the case for a small part of a given population.

5.5. Population heterogeneity

Low standard deviations of the measured bacterial zeta potentials (Table 3) (calculated with mean values of different electrophoretic mobility measurements from separate cultures) were obtained which suggest homogeneous electrophoretic characteristics for each strain. However each of our electrophoretic measurements is the average of at least 100 individual bacterial cells. In our case the standard deviation calculated from these individual measurements turned out to be up to 10 mV in some pure cultures (results not shown). Thus the standard deviations shown in Table 3 do not reflect the real ζ-potential distribution that can exist within a single strain microbial population. As van der Mei and Busscher [54] pointed out in their mini review the standard deviation calculated from individual electrophoretic cell measurements reflects a high degree of heterogeneity and may reveal the existence of subpopulations within a pure culture. Hence, cells from the same strain probably experience energy barriers with different intensities when approaching the solid. In consequence only a part of the population may be in conditions favorable for retention. This may also explain different adhesion rates for cells of the same strain during the experiments (Fig. 2).

5.6. Rate of adhesion

A correlation ($R^2 = 0.71$, $p < 0.0001$) was found between the ω parameter describing the rate of adhesion and the ΔG^{EL} of the strains studied (Fig. 3). This result indicates that high values of ΔG^{EL} can temporally prevent bacterial cells from approaching the solid phase close enough to be trapped. It should be kept in mind that ΔG^{EL} depends on the ζ potential of both the cells and the soil and also that the ζ potential of the cells is strongly linked to environmental factors such as the pH and the ionic strength of the soil solution. Several studies pointed out that ζ potential of living cells is lowered by higher ionic strengths (larger than 0.1 M NaCl) which eliminate the electrostatic barrier. In the same way most bacterial cells have isoelectric points below pH 4.0 [55]. Studies by the same author have shown that anionic groups dominate over cationic groups which mean that an increase of the pH of the environment would increase the ζ potential and thus ΔG^{EL}. However in soil environments ionic strengths are very often lower than 0.01 M and the pH is mild. So, in such conditions, electrostatic interactions should remain important and delay bacteria adhesion to the soil matrix, which is favourable to their transport through the porous medium.

6. Conclusions

In this study we investigated the influence of cell surface properties on attachment kinetics using the extended DLVO theory. Zeta potential of both the porous media and the bacterial cells played a significant role in bacterial adhesion behaviour through the sand matrix. Low zeta potentials resulted in electrostatic repulsions which delays bacterial adhesion. In such conditions bacterial transport is enhanced. Different adhesion behaviour onto sand between hydrophobic and hydrophilic cells was mainly due to AB interactions. Hydrophobic strains were better retained by the sand matrix than hydrophilic strains. However we could not relate cell retention to the free energy of interaction as calculated with the XDLVO theory. This failure has certainly many origins among which cell trapping by mechanisms in porous media not accounted for by the XDLVO theory. It appears that bacterial adhesion phenomena depends on both physicochemical interactions and porous media related effects.

Acknowledgements

This study was partly funded by the ADEME (French agency for Environment and Energy control) and the INRA (French National Institute for Agriculture Research). The authors thank E. Moustier for his help during the electrophoretic measurements and I. Bornard for her help providing the SEM pictures of sand grains.

References

[1] D.E. Fontes, A.L. Mills, G.M. Hornberger, J.S. Herman, Appl. Environ. Microbiol. 57 (1991) 2473.
[2] R.R.E. Artz, J. Townend, K. Brown, W. Towers, K. Killham, Environ. Microbiol. 7 (2005) 241.
[3] A. Unc, M.J. Goss, Appl. Soil Ecol. 25 (2004) 1.
[4] B.M. Brunninger, D.M.S. Mano, I. Scheunert, T. Langenbach, Ecotoxicol. Environ. Saf. 44 (1999) 154.
[5] J.F. McCarty, J.M. Zachara, Environ. Sci. Technol. 23 (1989) 496.
[6] S.B. Kim, M.Y. Corapcioglu, J. Contam. Hydrol. 59 (2002) 267.
[7] M.Y. Corapcioglu, S.H. Kim, Water Resour. Res. 31 (1995) 2639.
[8] T. Mattilasandholm, G. Wirtanen, Food Rev. Int. 8 (1992) 573.
[9] F. Celico, M. Varcamonti, M. Guida, G. Naclerio, Appl. Environ. Microbiol. 70 (2004) 2843.
[10] J.T. Gannon, V.B. Manilal, M. Alexander, Appl. Environ. Microbiol. 57 (1991) 190.
[11] M.C.M. van Loosdrecht, J. Lyklema, W. Norde, A.J.B. Zehnder, Microb. Ecol. (1989) 1.
[12] G. Chen, K.A. Strevett, Environ. Eng. Sci. 20 (2003) 237.
[13] K.C. Marshall, R. Stout, R. Mitchell, Can. J. Microbiol. 17 (1971) 1413.
[14] C.J. van Oss, Cell Biophys. 14 (1989) 1.
[15] C.J. van Oss, J. Mol. Recognit. 16 (2003) 177.
[16] B.F. Smets, D. Grasso, M.A. Engwall, B.J. Machinist, Coll. Surf. B 14 (1999) 121.
[17] C. Gomez-Suarez, J. Pasma, A.J. van der Borden, J. Wingender, H.C. Flemming, H.J. Busscher, H.C. van der Mei, Microbiology 148 (2002) 1161.
[18] N. Iwabuchi, M. Sunairi, H. Anzai, H. Morisaki, M. Nakajima, Coll. Surf. B 30 (2003) 51.
[19] S. Tsuneda, J. Jung, H. Hayashi, H. Aikawa, A. Hirata, H. Sasaki, Coll. Surf. B 29 (2003) 181.
[20] G. Chen, K.A. Strevett, Coll. Surf. B 28 (2003) 135.
[21] M.F. DeFlaun, S.R. Oppenheimer, S. Streger, C.W. Condee, M. Fletcher, Appl. Environ. Microbiol. (1999) 759.
[22] N.I. Abu-Lail, T.A. Camesano, Environ. Sci. Technol. 37 (2003) 2173.
[23] T.A. Camesano, B.E. Logan, Environ. Sci. Technol. 32 (1998) 1699.
[24] M.W. Becker, S.A. Collins, D.W. Metge, R.W. Harvey, A.M. Shapiro, J. Contam. Hydrol. 69 (2004) 195.
[25] T.H. Weiss, A.L. Mills, G.M. Hornberger, J.S. Herman, Environ. Sci. Technol. 29 (1995) 1737.
[26] C.J. Van oss, Coll. Surf. B 5 (1995) 91.
[27] G. Chen, K.A. Strevett, Environ. Microbiol. 3 (2001) 237.
[28] G. Chen, K.A. Strevett, J. Environ. Eng. 128 (2002) 408.
[29] G. Chen, H.L. Zhu, Coll. Surf. B 44 (2005) 41.
[30] S.E. Truesdail, J. Lukasik, S.R. Farrah, D.O. Shah, R.B. Dickinson, J. Colloid Interface Sci. 203 (1998) 369.
[31] B.K. Li, B.E. Logan, Coll. Surf. B 36 (2004) 81.
[32] C.H. Bolster, G.M. Hornberger, A.L. Mills, J.L. Wilson, Environ. Sci. Technol. 32 (1998) 1329.
[33] N. Tufenkji, J.A. Redman, M. Elimelech, Environ. Sci. Technol. 37 (2003) 616.
[34] G. Chen, M. Rockhold, K.A. Strevett, Res. Microbiol. 154 (2003) 175.
[35] C.J. van Oss, Interfacial Forces in Aqueous Media, Dekker, New York, 1994.
[36] D. Grasso, B.F. Smets, K.A. Strevett, B.D. Machinist, C.J. VanOss, R.F. Giese, W. Wu, Environ. Sci. Technol. 30 (1996) 3604.
[37] M. Elimelech, M. Nagai, C.H. Ko, J.N. Ryan, Environ. Sci. Tecnol. 34 (2000) 2143.
[38] M.N. BellonFontaine, J. Rault, C.J. vanOss, Coll. Surf. B 7 (1996) 47.
[39] H.H.M. Rijnaarts, W. Norde, E.J. Bouwer, J. Lyklema, A.J.B. Zehnder, Coll. Surf. B (1995) 5.
[40] A.R. Shashikala, A.M. Raichur, Coll. Surf. B 24 (2002) 11.
[41] H.C. Vandermei, J. Devries, H.J. Busscher, Appl. Environ. Microbiol. 59 (1993) 4305.
[42] F. Hamadi, H. Latrache, M. Mabrrouki, A. Elghmari, A. Outzourhit, M. Ellouali, A. Chtaini, J. Adh. Sci. Technol. 19 (2005) 73.
[43] C.J. van Oss, Coll. Surf. A 78 (1993) 1.
[44] M.C. van Loosdrecht, J. Lyklema, W. Norde, G. Schraa, A.J. Zehnder, Appl. Environ. Microbiol. 53 (1987) 1898.
[45] F. Huysman, W. Verstraete, Soil Biol. Biochem. 25 (1993) 83.
[46] J.A. Redman, S.L. Walker, M. Elimelech, Environ. Sci. Technol. 38 (2004) 1777.
[47] S.A. Bradford, S.R. Yates, M. Bettahar, J. Simunek, Water Resour. Res. 38 (2002), Art. No. 1327.
[48] S. Bhattacharjee, C.H. Ko, M. Elimelech, Langmuir 14 (1998) 3365.
[49] E.M.V. Hoek, G.K. Agarwal, J. Colloid Interface Sci. 298 (2006) 50.
[50] E.M.V. Hoek, S. Bhattacharjee, M. Elimelech, Langmuir 19 (2003) 4836.
[51] N. Tufenkji, G.F. Miller, J.N. Ryan, R.W. Harvey, M. Elimelech, Environ. Sci. Technol. 38 (2004) 5932.
[52] S.A. Bradford, J. Simunek, M. Bettahar, M.T. van Genuchten, S.R. Yates, Water Resour. Res. 42 (2006) (Art. No. W12S15).
[53] W.P. Johnson, X.Q. Li, G. Yal, Environ. Sci. Technol. 41 (2007) 1279.
[54] H.C. van der Mei, H.J. Busscher, Appl. Environ. Microbiol. 67 (2001) 491.
[55] A. van der Wal, W. Norde, A.J.B. Zehnder, J. Lyklema, Coll. Surf. B 9 (1997) 81.

Figures supplémentaires :

Par manque de place la figure 2 page 108 de l'article ne présente que les résultats du transport en colonne de sable des souches *E. coli* PHL565gfp, *Bacillus subtilis* et *S. salivarius* JIM8780. Les résultats des autres souches sont présentés ici.

Figure 10 : Figures supplémentaires

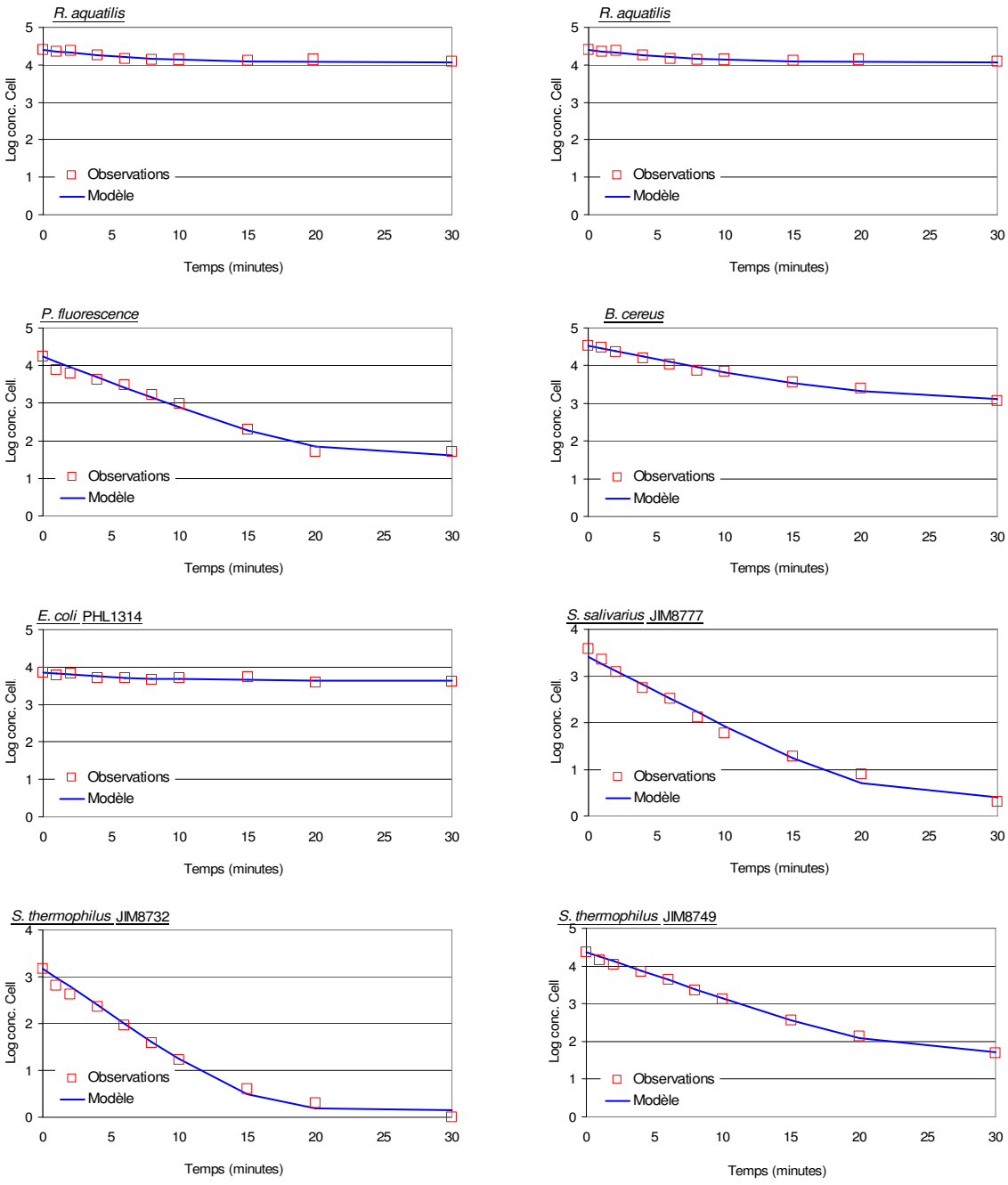

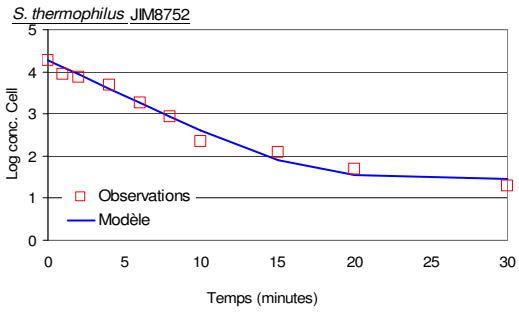

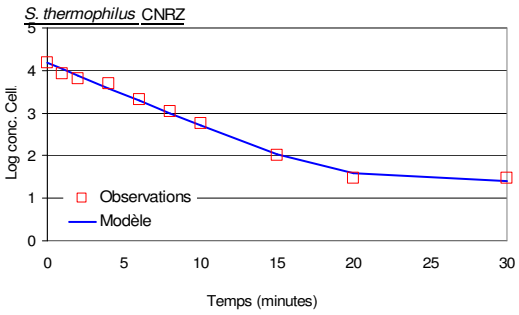

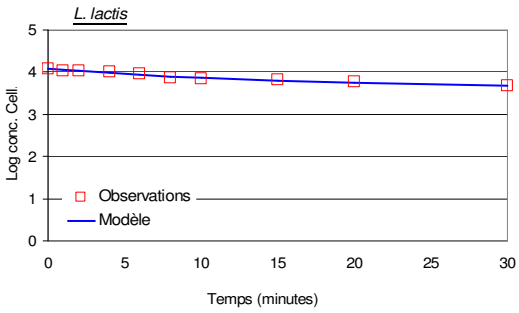

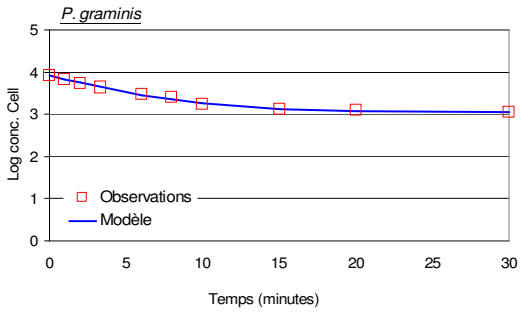

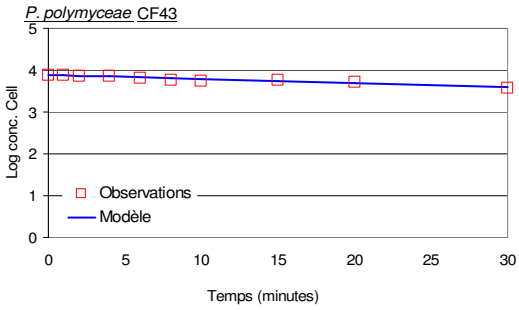

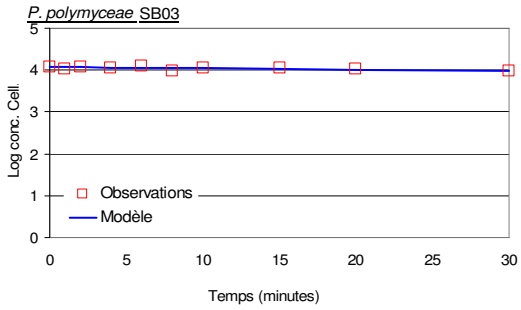

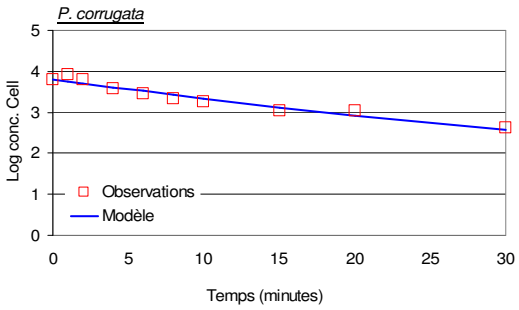

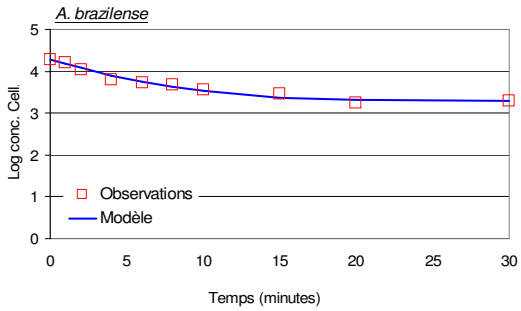

La figure 2 de l'article contient des valeurs erronées des résultats de la souche *S. salivarius* JIM8780, la figure en face correspond à la version corrigée :

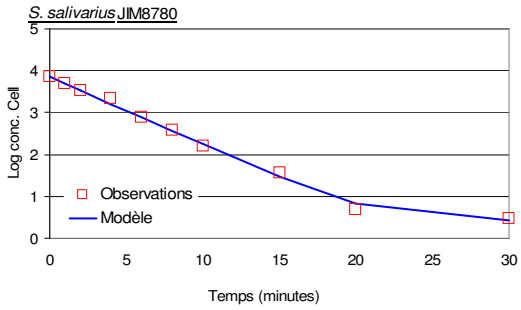

Précisions complémentaires :

Les souches *S. thermophilus* JIM8752, *S. thermophilus* JIM8749 et *S. thermophilus* CNRZ fabriquent des quantités d'EPS différents. Bien que non vérifiées par nos propres soins, selon le laboratoire de provenance (centre INRA Jouy en Josas, Paris, France) les souches JIM8752 (delta *epsE*) et JIM8749 (delta *epsB*) sont des mutants EPS de *S. thermophilus* CNRZ1066. Le mutant *epsE* ne produit pas d'EPS et le mutant *epsB* en produit 2 fois moins que la souche sauvage. Le mutant *epsB* a aussi une taille légèrement plus petite que la souche sauvage. Malgré ces caractéristiques physiologiques différentes, les mutants présentaient un comportement de transport dans le sable et des propriétés de surface presque identiques. Toutefois à cause de l'absence de quantification de la production d'EPS chez ces mutants pendant les expériences aucune interprétation n'a pu être faite.

Il en est de même pour les souches d*'E. coli* dont la quantité de curlis fabriquée est différente : la souche PHL1314 est un mutant (*omp*R 234) de la souche PHL565 et fabrique des curlis en plus grande quantité. Les curlis seraient impliqué dans la formation de biofilms et dans l'adhésion des bactéries sur des cellules épithéliales d'un organisme hôte. Mais l'absence de quantification de la production de curlis pendant les expériences ne permet pas de conclure sur un quelconque effet des curlis.